Jpn. J. Appl. Phys. Vol. 40 (2001) pp. 2721–2724
Part 1, No. 4B, April 2001

# A Low Voltage Actuated Microelectromechanical Switch for RF Application

Dooyoung HAH*, Euisik YOON and Songcheol HONG

*Department of Electrical Engineering and Computer Science, Korea Advanced Institute of Science and Technology (KAIST),
373-1 Kusong-dong, Yusong-gu, Taejon 305-338, Korea*

(Received August 28, 2000; accepted for publication November 15, 2000)

A push-pull operation is proposed for low voltage actuation of a microelectromechanical (MEM) switch for RF application. The push-pull operation realized by torsion springs and contact electrode height amplification by leverage, lowers the actuation voltage of the MEM switch by reducing the gap between actuation electrodes. The proposed MEM switch is fabricated by gold surface micromachining. Switching operation up to 4 GHz is demonstrated. The actuation voltage is as low as 5 V. The insertion loss of $\sim$ 1 dB and the isolation as high as $\sim$ 40 dB at 1 GHz are achieved by the push-pull operation.

KEYWORDS: microelectromechanical switch, RF switch, push-pull operation, leverage, gold surface micromachining

## 1. Introduction

Micromachining is expected to become a significant tool in RF communication systems. RF microelectromechanical (MEM) switches, in particular, have been paid great attention to due to their excellent electrical performance compared to their semiconductor counterparts, such as GaAs field effect transistors (FETs) and p-i-n diodes.[1–5] They show low insertion loss ($< 0.5$ dB) and high isolation ($> 30$ dB) characteristics in the range of microwave and millimeter waves. They do not exhibit intermodulation distortion (IMD). In addition, they have low power consumption characteristics and moderate switching speed. However, their main drawback is the high actuation voltage (typically, $> 20$ V) because most of them are actuated by electrostatic force. In most cases, the gap between the actuation electrodes is 3–4 $\mu$m for sufficient isolation in the off state. This results in the high actuation voltage in the RF MEM switches. One way to lower the actuation voltage while maintaining high isolation is to change the configuration. In this work, we demonstrate the low voltage actuated RF MEM switch by utilizing a push-pull configuration and leverage. In this paper we will discuss the operating principle, design issues, fabrication techniques, experimental results, and areas requiring further research.

## 2. Push-Pull Configuration

Figures 1(a) and 1(b) show the scanning electron microscope (SEM) image and the photograph of the proposed RF MEM switch, respectively. As described in §1, to achieve both high isolation and low actuation voltage we utilize the push-pull configuration. There are three actuation electrodes, which are composed of two fixed electrodes, a 'push' electrode and a 'pull' electrode, on the substrate and one rotating electrode floated over the substrate. When voltage is applied between the pull and the rotating electrodes (Fig. 2(a)), the contact electrode attached to the rotating electrode through the lever moves down to make contact with the signal line. When this pull voltage is eliminated and the voltage is applied between the push and the rotating electrodes (Fig. 2(b)), the contact electrode is lifted upward. Moreover, the contact electrode height ($h_c$) in the off state is amplified by the leverage, which is expressed as,

$$h_c = \left(2 + \frac{l_{\text{lever}}}{l_{\text{re}}}\right) h_0, \qquad (1)$$

where, $l_{\text{lever}}$ is the length of the lever, $l_{\text{re}}$ is the half length of the rotating electrode, and $h_0$ is the initial contact electrode height. This shows that $h_c$, hence the isolation, increases as

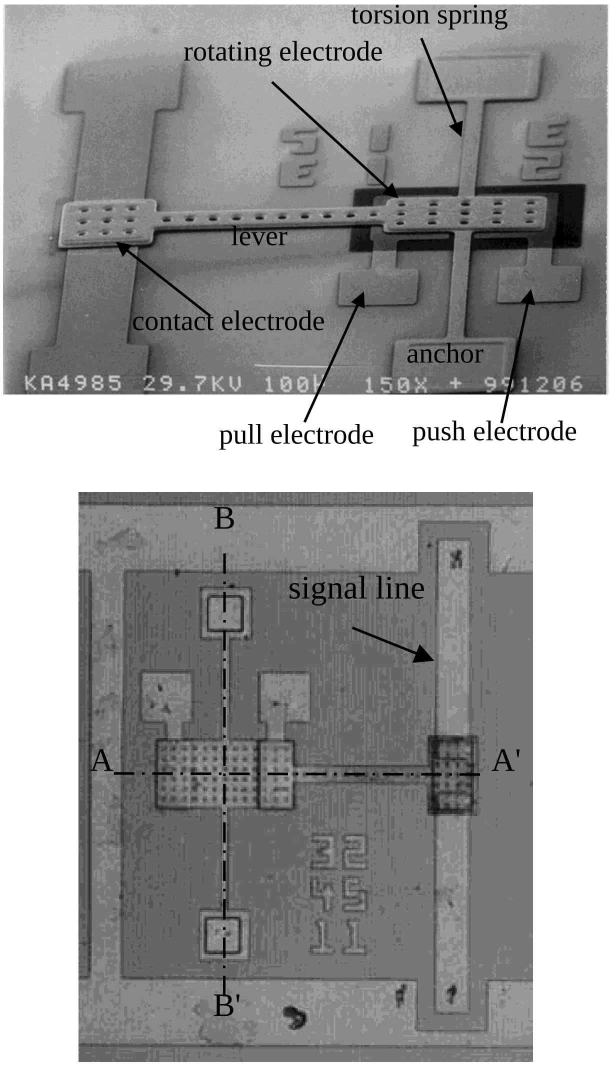

Fig. 1. (a) The SEM image and (b) the photograph of the proposed RF MEM switch using a push-pull configuration.

---

*Present address: Department of EE, UCLA, Los Angeles, CA 90095-1594, USA; E-mail address: hady@icsl.ucla.edu

$l_{\mathrm{lever}}$ increases. Therefore, we can reduce the actuation voltage by lowering $h_0$ while maintaining the high isolation.

## 3. Design

The actuation voltage is determined by the geometrical dimensions and the material properties of the torsion springs and the rotating electrode. Gold is selected as the main structural material due to its low shear modulus and low residual stress. Since switching is carried out by electrostatic torque, one has to know the relationship between electrostatic torque ($T_{\mathrm{e}}$) and rotation angle ($\theta$) to estimate the actuation voltage. That is,

$$T_{\mathrm{e}}(\theta) = \frac{\varepsilon_0 V^2 w_{\mathrm{re}}}{2\sin^2\theta}\left[\frac{l_{\mathrm{re}}\sin\theta}{h_0 - l_{\mathrm{re}}\sin\theta + t_{\mathrm{d}}/\varepsilon_{\mathrm{d}}} + \ln(h_0 - l_{\mathrm{re}}\sin\theta + t_{\mathrm{d}}/\varepsilon_{\mathrm{d}}) - \frac{(l_{\mathrm{re}} - l_{\mathrm{fe}})\sin\theta}{h_0 - (l_{\mathrm{re}} - l_{\mathrm{fe}})\sin\theta + t_{\mathrm{d}}/\varepsilon_{\mathrm{d}}} - \ln(h_0 - (l_{\mathrm{re}} - l_{\mathrm{fe}})\sin\theta + t_{\mathrm{d}}/\varepsilon_{\mathrm{d}})\right], \tag{2}$$

where, $V$ is the applied voltage, $w_{\mathrm{re}}$ is the width of the rotating electrode, and $l_{\mathrm{fe}}$ is the length of one of the fixed electrodes.[6] $t_{\mathrm{d}}$ and $\varepsilon_{\mathrm{d}}$ are the thickness and the dielectric constant of the insulator beneath the rotating electrode, respectively. At equilibrium, $T_{\mathrm{e}}$ is equal to the restoring torque ($T_{\mathrm{r}}$), which can be given as:

$$T_{\mathrm{r}}(\theta) = \frac{2GJ\theta}{l_{\mathrm{s}}}, \tag{3}$$

where, $l_{\mathrm{s}}$ and $G$ are the length and the shear modulus of the torsion springs, respectively. $J$ is the polar moment of inertia of the springs, which is expressed as,

$$J = \frac{w_{\mathrm{s}} t_{\mathrm{s}}}{12}(w_{\mathrm{s}}^2 + t_{\mathrm{s}}^2), \tag{4}$$

where, $w_{\mathrm{s}}$ and $t_{\mathrm{s}}$ are the width and the thickness of the torsion springs, respectively.[7] One can obtain the relationship between $\theta$ and $V$ by solving the equation,

$$T_{\mathrm{e}}(\theta) = T_{\mathrm{r}}(\theta). \tag{5}$$

When $V$ is small, there exists a solution. However, above a threshold voltage ($V_{\mathrm{th}}$), eq. (5) cannot be solved. This means that the rotating electrode is abruptly pulled down to touch the fixed electrode at $V_{\mathrm{th}}$. Figure 3 shows the calculated relationship between $V$ and $\theta$. In this case, $V_{\mathrm{th}}$ is 3.5 V. The off-voltage ($V_{\mathrm{push}}$) is $V_{\mathrm{th}}$ because the rotating electrode directly touches the push electrode. The on-voltage ($V_{\mathrm{pull}}$) can be lower than $V_{\mathrm{th}}$ because the contact electrode can be brought in contact with the signal line before the rotating electrode is brought in contact with the pull electrode. Therefore, the overall actuation voltage of the switch is estimated to be $V_{\mathrm{th}}$. The various dimensions of the torsion springs and the electrodes were designed to examine the relationship between the dimensions and the actuation voltages. The length of the torsion spring ($l_{\mathrm{s}}$) was designed from 100 $\mu$m to 500 $\mu$m. The width of the torsion spring ($w_{\mathrm{s}}$) was varied between 10 $\mu$m and 20 $\mu$m. The thickness of the torsion spring was designed to be 1.4 $\mu$m. The half length of the rotating electrode ($l_{\mathrm{re}}$) was designed from 100 $\mu$m to 400 $\mu$m.

The contact area has to be designed carefully to achieve good RF performance. As the contact area increases, on-resistance ($R_{\mathrm{on}}$) decreases and off-capacitance ($C_{\mathrm{off}}$) increases. The designed contact area was 90 × 90 $\mu$m$^2$. The signal line gap was designed to be 20 $\mu$m.

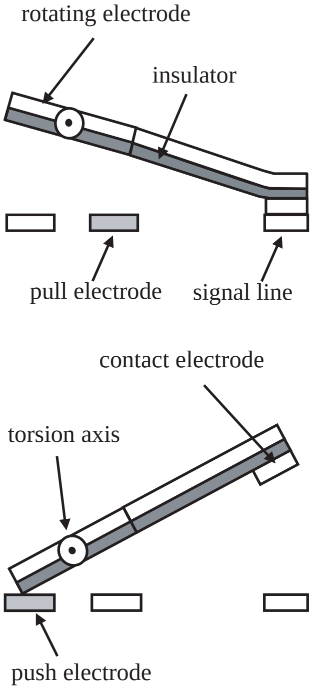

Fig. 2. The proposed push-pull configuration (a) at the on state (when $V_{\mathrm{pull}}$ is on) and (b) at the off state (when $V_{\mathrm{push}}$ is on).

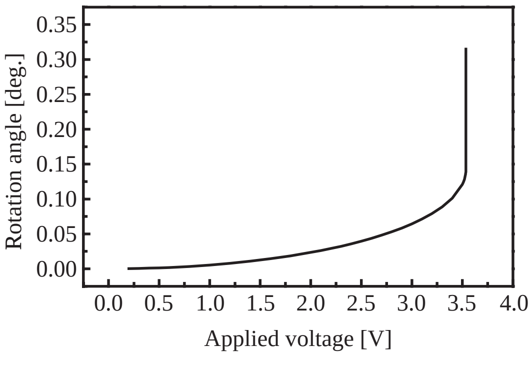

Fig. 3. The calculated relationship between the applied voltage and the rotation angle of the rotating electrode.

## 4. Fabrication

Figure 4 shows the fabrication process of the RF MEM switch. Semi-insulating GaAs is used as the substrate. Other insulating materials, such as alumnia, high resistivity Si and Quartz, can also be used. First, the signal line and the fixed (push and pull) electrodes are formed by gold plating (Fig. 4(a)). AZ5214 photoresist is spun as a sacrificial layer and the anchors are defined. The contact electrode is formed by

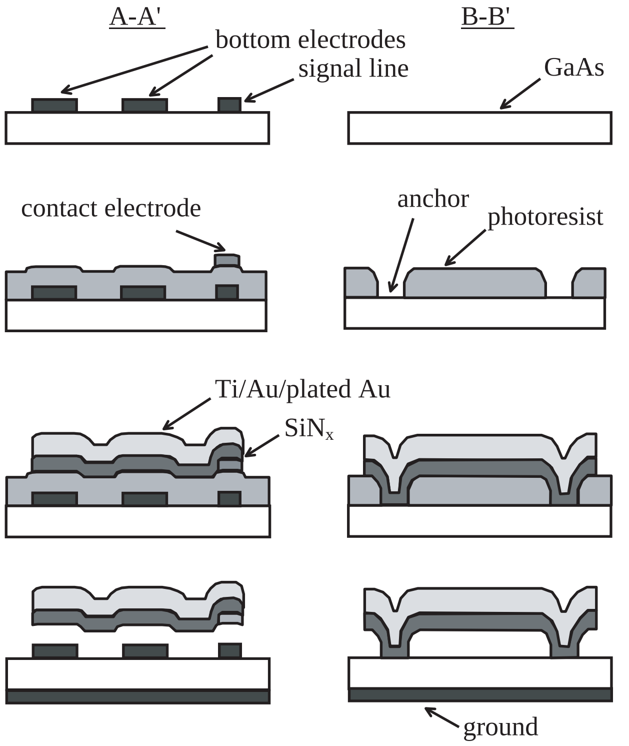

Fig. 4. The fabrication process of the RF MEM switch: (a) formation of the bottom electrodes and signal line; (b) sacrificial layer and contact electrode formation; (c) structure layer formation; and (d) structure release.

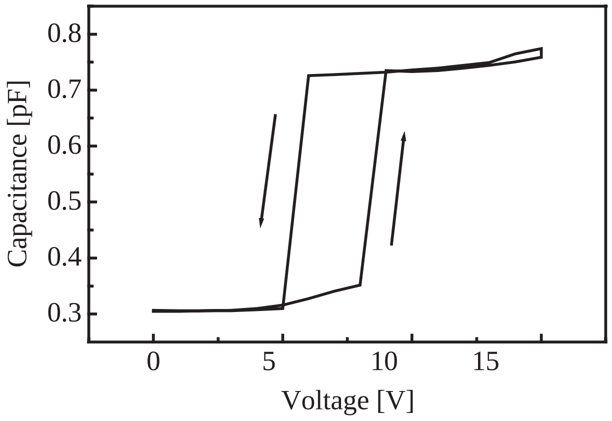

Fig. 5. The $C$–$V$ measurement result between the actuation electrodes of the fabricated RF MEM switch (torsion spring: $1.4\,\mu\text{m}(t) \times 10\,\mu\text{m}(w) \times 300\,\mu\text{m}(l)$, $l_{\text{re}}$: $200\,\mu$m).

gold plating (Fig. 4(b)). The movable structure is formed as a multilayer of SiN$_x$ (0.2 $\mu$m)-titanium/gold (20/50 nm)-plated gold (1.1 $\mu$m) as a stress compensated structure (Fig. 4(c)). Finally, the structure is released by O$_2$ plasma dry etching to prevent stiction problem (Fig. 4(d)).

## 5. Experiment Results

The capacitance–voltage ($C$–$V$) measurement result between the actuation electrodes of the fabricated switch (torsion spring: $1.4\,\mu\text{m}(t)\times 10\,\mu\text{m}(w)\times 300\,\mu\text{m}(l)$, $l_{\text{re}}$: $200\,\mu$m) is depicted in Fig. 5. It shows the abrupt change of the capacitance at the threshold voltage (in this case, 8 V). The initial upward deflection due to the residual stress gradient in the torsion springs was observed when $w_{\text{s}}$ was $10\,\mu$m. Hence, $V_{\text{th}}$ of the device in which $w_{\text{s}}$ is $10\,\mu$m was measured to be higher than $V_{\text{th}}$ of the device in which $w_{\text{s}}$ is $20\,\mu$m. Figure 6 shows the measured $V_{\text{pull}}$ and $V_{\text{push}}$ and the calculated $V_{\text{th}}$ according to the various values of $l_{\text{re}}$ when $l_{\text{s}}$ is $300\,\mu$m and $w_{\text{s}}$ is $20\,\mu$m. This shows that the actuation voltage decreases as $l_{\text{re}}$ increases. Figure 7 exhibits the measured $V_{\text{pull}}$ and $V_{\text{push}}$ and the calculated $V_{\text{th}}$ according to the various values of $l_{\text{s}}$ when $l_{\text{re}}$ is $200\,\mu$m and $w_{\text{s}}$ is $20\,\mu$m. This shows that the actuation voltage does not vary significantly with $l_{\text{s}}$. This may be caused by the residual stress of the torsion springs because the residual stress enlarges the spring constant and it becomes a more significant factor to $V_{\text{th}}$ as $l_{\text{s}}$ increases. There are some differences between the calculated $V_{\text{th}}$ and the measured $V_{\text{push}}$ as shown in Figs. 6 and 7. The reason for this is that the residual stress was not considered in the calculation performed in §3 for the sake of simplicity. The calculated $V_{\text{th}}$ according to the various $h_0$ and $t_{\text{s}}$ values is depicted in Fig. 8. It is shown that $V_{\text{th}}$ is significantly changed by $h_0$. On the basis of these results, it appears that the most effective way to reduce the actuation voltage is by decreasing $h_0$ and the proposed push-pull configuration is one of the ways to realize it. The minimum actuation voltage was measured to be 5 V. The closure time of the switch was measured to be 0.6 ms. The RF characteristics from 500 MHz to 4 GHz of the fabricated switch were

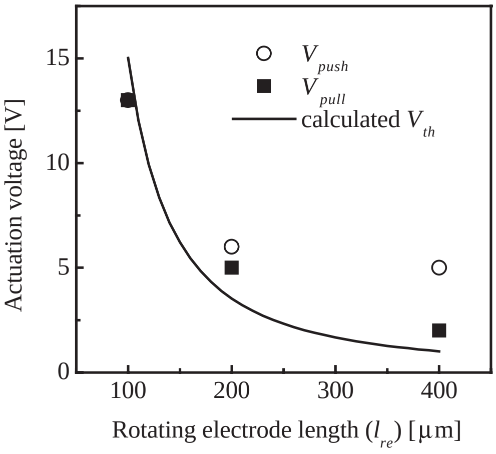

Fig. 6. The measured $V_{\text{pull}}$ and $V_{\text{push}}$ and the calculated $V_{\text{th}}$ according to the various $l_{\text{re}}$ values (when $l_{\text{s}}$ is $300\,\mu$m and $w_{\text{s}}$ is $20\,\mu$m).

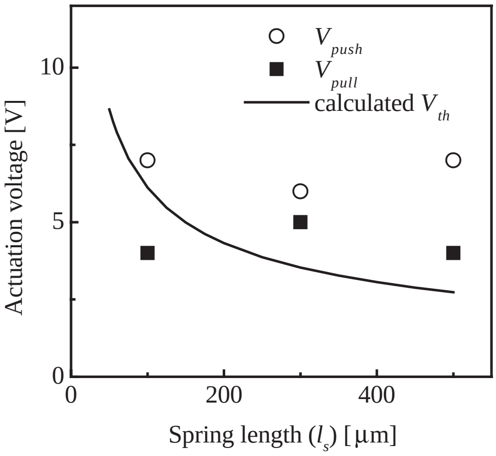

Fig. 7. The measured $V_{\text{pull}}$ and $V_{\text{push}}$ and the calculated $V_{\text{th}}$ according to the various $l_{\text{s}}$ values (when $l_{\text{re}}$ is $200\,\mu$m and $w_{\text{s}}$ is $20\,\mu$m).

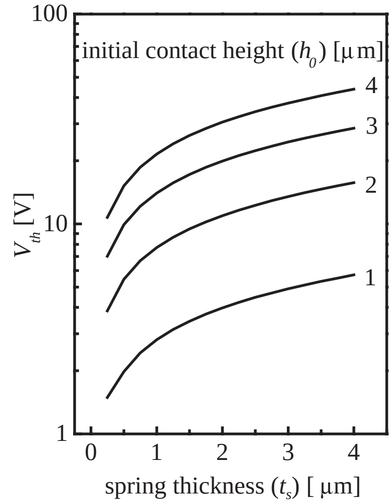

Fig. 8. The calculated $V_{\text{th}}$ according to the various $h_0$ and $t_s$ values.

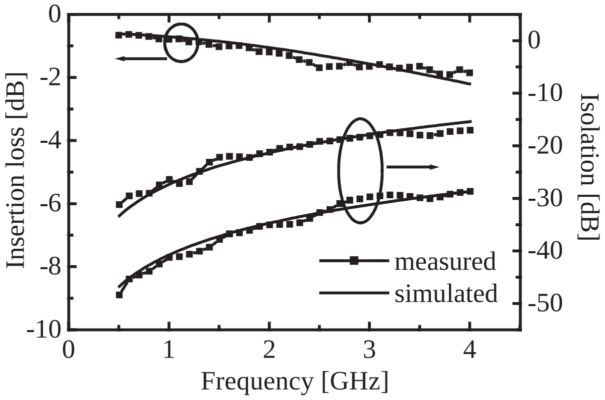

Fig. 9. The measured (line+square) and simulated (line) RF characteristics of the fabricated RF MEM switch.

examined using a HP8720C network analyzer (Fig. 9). The insertion loss was below 1 dB up to 2 GHz and 2 dB up to 4 GHz. This relatively large insertion loss may be due to the parasitic capacitance between the contact electrode and the rotating electrode and high $R_{\text{on}}$ measured as 8 Ω. The reason for this high $R_{\text{on}}$ may be that a hard contact is not formed because of the distance between the pull electrode and the contact electrode. At zero bias, the isolation was measured to be $>$ 17 dB up to 4 GHz. It became $>$ 28 dB in the push operation, improving the isolation by $\sim$ 10 dB. The isolation will be further improved with a wider signal line gap. $C_{\text{off}}$ was 70 fF at zero bias and reduced to 15 fF in the off state.

## 6. Conclusions

A surface-micromachined RF switch with a push-pull configuration has been demonstrated. The actuation voltage of as low as 5 V has been achieved by means of torsion springs and leverage. From the experimental results, it was proven that the most effective way to reduce the actuation voltage is by decreasing the gap ($h_0$) between the actuation electrodes and the push-pull operation is one of the ways to realize it. The RF characterization showed that the isolation can be significantly improved by the push-pull configuration. This switch can be used for mobile RF telecommunication systems.

## Acknowledgements

This work is partially supported by the National Research Laboratory project and The Millimeter-wave Innovation Technology research center. The authors would like to thank D. Baek, M. Kim, E. Park and Y. Kang at KAIST for their help with the fabrication process.

1) J. J. Yao and M. F. Chang: Proc. 8th Int. Conf. Solid-State Sens. Actuators and Eurosensors IX (1995) p. 384.
2) C. Goldsmith, Z. Yao, S. Eshelman and D. Denniston: IEEE Microwave and Guided Wave Lett. **8** (1998) 269.
3) D. Hyman, A. Schmitz, B. Warneke, T. Y. Hsu, J. Lam, J. Brown, J. Schaffner, A. Walston, R. Y. Loo, G. L. Tangonan, M. Mehregany and J. Lee: Electron. Lett. **35** (1999) 224.
4) J. B. Muldavin and G. M. Rebeiz: Proc. IEEE MTT-S Symp. (1999) p. 1511.
5) J. Park, G. Kim, K. Chung and J. Bu: Proc. 13th Int. IEEE MEMS Conf. (2000) p. 384.
6) H. Toshiyoshi and H. Fujita: IEEE J. Microelectromech. Syst. **5** (1996) 231.
7) J. M. Gere and S. P. Timoshenko: *Mechanics of Materials* (PWS Publishing Company, Boston, 1997) 3rd ed., p. 868.